Article

Heterogeneous Growth of Metal Clusters from Solutions of Seed Nanoparticles

Jess Patrick Wilcoxon, and Paula P. Provencio

J. Am. Chem. Soc., **2004**, 126 (20), 6402-6408• DOI: 10.1021/ja031622y • Publication Date (Web): 01 May 2004

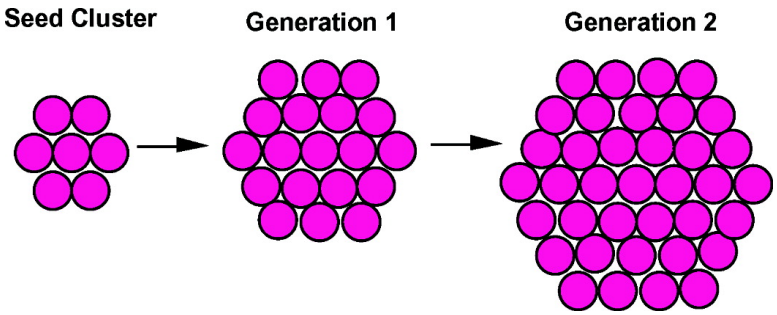

More About This Article

Additional resources and features associated with this article are available within the HTML version:

- Supporting Information
- Links to the 8 articles that cite this article, as of the time of this article download
- Access to high resolution figures
- Links to articles and content related to this article
- Copyright permission to reproduce figures and/or text from this article

View the Full Text HTML

J|A|C|S
ARTICLES
Published on Web 05/01/2004

Heterogeneous Growth of Metal Clusters from Solutions of Seed Nanoparticles

Jess Patrick Wilcoxon* and Paula P. Provencio

Contribution from the Nanostructures and Advanced Materials Chemistry, Department 1122, Sandia National Laboratories, Albuquerque, New Mexico 87185-1421

Received December 10, 2003; E-mail: jpwilco@sandia.gov

Abstract: We describe the solution growth of a series of discrete sized generations of Au nanoparticles by the heterogeneous deposition of atoms onto monodisperse seed nanocrystals. The growth process was studied using size-exclusion chromatography (SEC) and transmission electron microscopy (TEM). The size dispersion of each generation was determined from the SEC elution line widths and the spectral homogeneity of the elution peaks. The heterogeneous deposition of various amounts of Ag on Au nanocrystals and Au on Ag nanocrystals using the same synthetic protocol is also described. The effect of such deposition on the optical absorbance of each generation of larger clusters was measured during SEC using an on-line photodiode array absorbance detector.

I. Introduction

The understanding and control of crystal growth are critical to modern science and technology. A general strategy for producing high quality crystals is to maintain the growth solution slightly supersaturated in the atomic or molecular species to be deposited so that the lowest energy equilibrium positions can be attained. Often modifiers (e.g., surfactants) are added to moderate the growth rate or influence the final crystal habit.

Growth of nanocrystals in solution also relies on surfactants to control unwanted cluster aggregation during chemical reduction of ionic precursors or thermal decomposition of metal-organics. In the case of chemical reduction of a metal salt, for example, the nucleation event may be localized uniformly in space and time by the presence of nanometer size cavities (e.g., zeolites) or by creating a microheterogeneous solution. The latter strategy is the basis for nanocrystal growth in the interior of surfactant aggregates (micelles or vesicles). In both cases, the diffusion of new material and its deposition onto the seed nuclei will be much slower than would occur in a continuous phase such as a liquid or gas. In the latter case, the aggregation kinetics as described by the Smoluchowski equation predicts a power-law (or log-normal) size distribution in the final product. Such strong polydispersity is generally unwanted.

In the case of slow, controlled growth of small nanocrystals in a microheterogeneous environment, one anticipates that facile surface diffusion of atoms deposited on the initial nuclei may create structures controlled by thermodynamic considerations rather than kinetic ones as in classical colloidal growth. As the growing clusters undergo diffusion and collisions in the solution, intercluster exchange of atoms may even occur in order to achieve a structure with the most thermodynamically stable structure. Some indications of this tendency have been reported in the solution growth of Ir clusters as reported by Watzky and Finke[1]

In the case of small clusters observed in cluster beam experiments, such "magic" sizes are well established, though they do not exist in overwhelming abundance. Whether solution growth favors such special sizes is an open question, though the pioneering work of G. Schmid on Au($N = 55$ atoms) demonstrates that it might.[2] Recent work[3] indicates that especially stable sizes are favored in both thiol etching processes and growth of nanoclusters using inverse micelles.

We first describe the synthesis and characterization of the seed nanocrystals using inverse micelles.[4−6] In the present studies we utilized high-resolution size-exclusion chromatography (SEC) to study the size dispersion of the clusters formed, as negligible polydispersity is required for successful growth of further generations of particles.[7,8]

We describe a heterogeneous growth process in which an organo-metallic source of atoms is slowly coinjected with a solution containing a metal hydride reductant into a stirred vial containing the nanocluster seed crystals. Metal atoms from this coinjection are deposited onto the surface of the seed nanoclusters, growing several generations of clusters by using each generation as the source of seeds for the growth of the next larger generation. A similar growth method was described by Klabunde and co-workers for the case of Co clusters.[9]

We first demonstrate this growth process for the case of homoatomic deposition of Au on Au nanocrystals for three

(1) Watzky, M. A.; Finke, R. G. *Chem. Mater.* **1997**, *9*, 3083.
(2) Schmid, G. *Angew. Chem.* **1978**, *90*, 417.
(3) Wilcoxon, J. P.; Provencio, P. *J. Phys. Chem. B* **2003**, *107*, 12949.
(4) Wilcoxon, J. P. Method for the Preparation of Metal Colloids in Inverse Micelles and Product preferred by the method. U.S. Patent 5,147,841, issued Sep. 15, 1992.
(5) Wilcoxon, J. P.; Martino T.; Klavetter, E.; Sylwester, A. P. Synthesis and Catalytic Properties of Metal and Semiconductor Nanoclusters. In *Nanophase Materials;* Hadjipanaysis and Siegel, Eds.; 1993; pp 770−780.
(6) Wilcoxon, J. P.; Williamson, R. L.; Baughman, R. J. *J. Chem. Phys.* **1993**, *98*, 9933.
(7) Wilcoxon, J. P.; Martin, J. E.; Provencio, P. *Langmuir* **2000**, *16*, 9912.
(8) Wilcoxon, J. P.; Martin, J. E.; Provencio, P. *J. Chem. Phys.* **2001**, *115*, 998.

10.1021/ja031622y CCC: $27.50

different growth rates, comparing the observed sizes to those expected for complete deposition of the reduced atoms onto the spherical nanocrystal seeds. We show that simple growth models involving only mass conservation adequately describe our results.

We also demonstrate the deposition of Ag on Au nanocrystals and Au on Ag nanocrystal seeds. In the core/shell structures of the latter two cases, we use an on-line photodiode array detector to monitor the changes in the absorbance as additional layers of atoms are deposited onto the seed nanocrystals.

II. Experimental Section

Synthesis. To provide seed nanocrystals for our heterogeneous growth experiments, we require very small ($D < 2$ nm), nearly perfect nanocrystals with a narrow size dispersion. Such nanocrystals can be produced by a chemical reduction of metal salts in the interior of inverse micelles.[4]

Since we wish to deposit additional atoms onto the surfaces of these seeds, a somewhat labile ligand must be employed to prevent aggregation. We also require a source of atoms which can be chemically reduced in a nonpolar organic solvent but which will have a low probability of forming atomic clusters which could act as competing nucleation centers. For the latter requirement, we chose to use metal organic chemicals, many of which are soluble in either benzene or toluene.

The Au or Ag seed particles were synthesized by $LiAlH_4$ reduction of $NaAuCl_4$ in a cationic or nonionic surfactant inverse micelle solution as has been described previously.[8] The monodispersity of the seed nanocrystals is critical if a narrow size dispersion is to be retained in each successive growth generation.

All reactions were performed in an Ar-filled vacuum atmospheres glovebox due to the air-sensitive nature of the reducing agents used. Synthesis of the $D = 1.8$ nm Au seed particles used a 10 wt % solution of the nonionic surfactant pentaethyleneglycol mono-*n*-dodecyl ether (C12E5) in hexadecane (C16) containing 0.01 M HAuCl4 and 0.01 M dodecanethiol (C12SH). This solution is chemically reduced under inert atmosphere using a 1 M stock solution of $LiAlH_4$ in tetrahydrofuran (thf). The final Au(III):AlH_4 ratio was 1:4. The orange colored nanoclusters are then precipitated using anhydrous methanol and dissolved in benzene. Size-exclusion chromatography shows them to have a very narrow size distribution of 1.8 ± 0.1 nm.[7] Yields of this synthesis and purification were 80−90% as determined by X-ray fluorescence (XRF) concentration measurements.

Ag nanocluster seeds with a size of $D = 2.4$ nm were synthesized in the two-component cationic inverse micelle consisting of 5 wt % tetraoctylammonium chloride (TOAC) containing 0.01 M $Ag(BF_4)_2$. This solution was reduced by addition of $LiBH_4$ (1 M stock in thf) with a final [Ag]:[BH_4] ratio of 0.02. Since Ag clusters are more oxygen-sensitive than Au, purification of the clusters via precipitation was done under anaerobic conditions and the purified seeds were used within a week of synthesis.

In all examples given below, an alkanethiol at a concentration ratio of [Metal]:[Thiol] = 5:1 was used to stabilize the nanocrystals during the deposition of the atoms from the metal-organic feedstock. The same molar ratio was used in this feedstock.

Transmission Electron Microscopy. Bright field TEM was used on a JEOL EX at 120 kv with a point-to-point resolution of approximately 9 Å. Magnifications of 50 kX or 100 kX were used to obtain diffraction contrast images. A JEOL 2010 was used to obtain high-resolution lattice fringe images at magnifications of 600 kX or 800 kX. An ~2 μL drop of a ~0.01 M (atomic molarity) cluster solution in toluene is applied to a holey carbon grid which rests on absorbent filter paper which rapidly wicks away the solvent, allowing the clusters to be well dispersed on the grid.

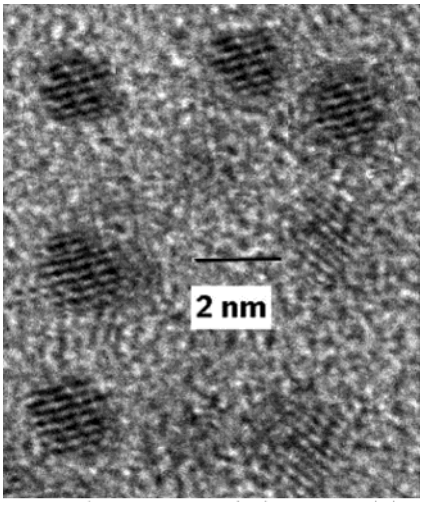

Figure 1. HRTEM of the Au seed nanoparticles used in the growth experiment.

X-ray Fluorescence. The Au and Ag seed concentrations were determined by X-ray fluorescence (XRF) against known, NIST traceable standards in the same organic matrix, toluene, using a QuantX XRF instrument.

Size-Exclusion Chromatography. A Water's Corporation Delta-prep commercial high-pressure liquid chromatograph equipped with an automated injector (model 717), and two detectors, a photodiode array, PDA, absorbance spectrometer (model 996) and a differential refractive index, RI, detector (model 410), were used to detect elution of the nanoclusters and nonabsorbing organic chemicals, respectively. A high-resolution Polymer's laboratory model PL1000 cross-linked polystyrene column filled with 5 μm microgel particles with dimensions of 7.8 (diameter) × 250 (length) mm^2 was used to separate the nanoparticles. The calibration of this system with size standards has been described previously in two papers, where it was demonstrated that, in the absence of specific chemical interactions between the cluster and the column, the time, t, required for elution is related to the hydrodynamic diameter, D_h, of the cluster by $\log D_h \approx t$.[7]

The hydrodynamic diameter is the sum of the inorganic core size as measured by TEM and the effective thickness of the organic shell in the mobile phase, toluene. The alkanethiol added to the mobile phase stabilizes the nanoclusters against aggregation during the chromatography. Its thickness for various chain length alkanethiols in toluene was previously determined as described in ref 7.

III. Results

Characterization of the Seed Particles. The size dispersion of each nanocluster generation grown by deposition of additional atoms onto the seed nanocrystals is critically dependent on the monodispersity of these seeds. Figure 1 shows an image by high-resolution TEM of a few nanocrystals from a small region of a holey carbon grid. Counting the lattice fringes for the crystals with orientations in the ⟨111⟩ direction and using the measured 2.34 Å fringe spacing show the particles to have a cross-sectional area of 8 ± 1 fringes or 1.9 ± 0.2 nm.

Figure 2 shows elution of these nanocrystals from a size-exclusion column (Polymer Labs, model PL1000) whose size calibration we have previously described.[7] Coplotted with this figure is the elution of a pure hydrocarbon decane. In both cases, the mobile phase was toluene containing 0.01 M dodecanthiol (C12SH), a mobile phase additive which improves the symmetry

(9) Lin, X. M.; Sorensen, C. M.; Klabunde, K. J.; Hajupanayis, G. C. *J. Mater. Res.* **1999**, *14*, 1542.

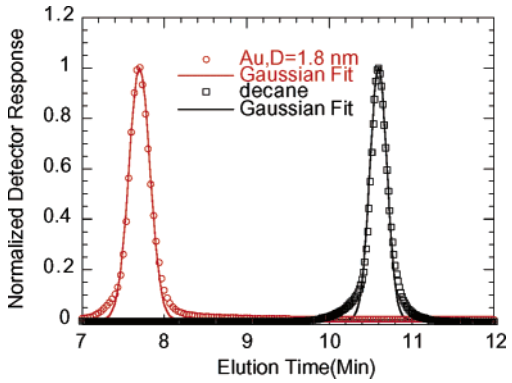

Figure 2. Chromatogram of the elution of the seed nanoparticles coated with dodecane thiol, compared to a reference monodisperse hydrocarbon, decane. The mobile phase was toluene flowing at 1 mL/min.

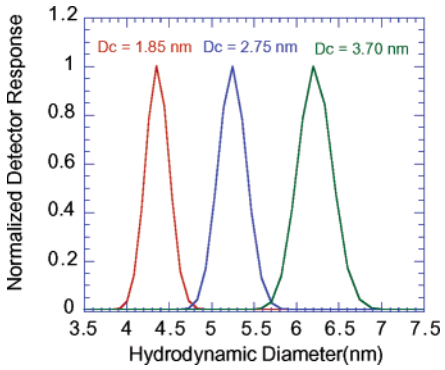

Figure 3. Hydrodynamic diameter as determined by SEC vs normalized detector response at 500 nm for seed nanoclusters with a core diameter of $D_c = 1.85$ nm and two growth generations. The molar ratio of Au in the seed clusters to that deposited on their surface was 1:2.

of the elution profile of the nanoclusters. The fit of the elution profile to a Gaussian is adequate and demonstrates that the inherent instrumental line width standard deviation (full-width at the 1/e point) is 0.30 ± 0.03 min. The uncertainty arises primarily from the chosen interval of 0.03 min between absorbance spectra. This is the time required to collect a full absorbance profile from 295 to 795 nm with a resolution of 2.4 nm using our on-line photodiode array (PDA). The line width of the seed particles is slightly larger at 0.36 min but significantly smaller than purified, 99.5% c60, (Strem Chemicals) with a line width of 0.56 min.

We make the conservative assumption that the minimum line width observed from the pure solvent reflects the inherent instrument response, even for the case of inorganic clusters passivated with organic groups, and deconvolute all our elution line shapes using a Gaussian instrumental function with this width.

Solution Epitaxial Growth on Seed Nanocrystals. Two gastight syringes were loaded with the organometallic feedstock and reducing agent, respectively, and independent syringe pumps (KD Scientific, model 100) were programmed to deliver these reagents at a typical rate of 2 mL/hr. Small inner diameter (∼.02 inch) Teflon tubes deliver the reagents from each syringe into a vial whose septa cap is penetrated by stainless steel needles attached to the end of the two tubes. The solution is stirred actively during the synthesis. The concentration of the nanocluster seeds is typically 0.01 M (in Au atoms), although concentrations as high as 0.1 M could be used, limited only by the solubility of the precursor organometallic reagents and the seed nanoclusters.

The specific metal to be deposited will determine the concentration and chemical type of surfactant used to control the growth. However, inverse micelle solutions of ionic metal salts should generally *not be used* as the source of atoms in the feedstock as the micelles can provide alternative nucleation centers for homogeneous growth of new nanocrystals. Instead, metallo-organic solutions are used, for example, Au(I) triphenyl phosphine chloride which is soluble in benzene. This reagent was selected, since reducing it with $LiBH_4$ or $LiAlH_4$ in the absence of seed nanocrystals results in the formation of an Au film on the glass.[3] We reasoned that the presence of large numbers of high surface area seed nanocrystals would favor deposition of the atoms onto the nanocrystals rather than the glass, and this proved correct. By adjusting the initial concentration of the seed nanoparticles and the total number of atoms injected, we can grow successive generations of particles of larger size at any desired rate.

We now describe the results of three specific growth experiments. Deposition of Au atoms onto $D = 1.8$ nm Au seeds at three different rates, deposition of Au onto Ag nanoclusters, and deposition of Ag onto Au nanocrystal seeds.

Heterogeneous Deposition of Au Atoms onto Au Nanocrystal Seeds. To illustrate the synthetic method, we consider the case of deposition of Au atoms onto Au seed nanoclusters. A metal-organic source of Au atoms, gold triphenyl phosphine chloride ($Au(PPh_3)Cl$) (0.01M in benzene), containing a stabilizer, dodecanethiol at 0.002 M, is drawn into one 10 mL gastight syringe. A reducing solution of $NaBH_4$ (0.04 M) is drawn into a second 10 mL syringe, and 2 mL of both samples are coinjected into a rapidly stirred vial containing 1 mL of the 0.01 M, $D = 1.8$ nm Au seed nanoparticles at an injection rate of 2 mL/hr. After an hour, one Au atom has been deposited for every two atoms in the seed clusters. A red shift in the color of the solution corresponding to growth of larger Au nanocrystals by deposition of Au atoms was observed. A 2 mL aliquot of this generation 1 growth solution is then removed for characterization by TEM and SEC, and the process was continued 2 more times with each larger generation of nanocrystal seeds serving as the starting solution for the next growth generation.

We also performed solution deposition using the 0.01 M, $D = 1.8$ nm seed nanoparticle solution but injected a smaller volume of metallo-organic feedstock solution, obtaining a 1:1 and 2:1 Au(seed):Au(deposited) ratio for the first growth generation. This permits a determination of the effect of depositing fewer atoms per growth generation on the observed size. These growth experiments were continued for six or seven generations. Attempts to grow clusters larger than ∼7−8 nm using monodentite alkanethiol stabilizers in the growth medium failed due to aggregation of the clusters. We have, however, recently developed block copolymer stabilizers which may allow this growth process to be continued to much larger cluster sizes.

Characterization of the Growth Process. The injected Au(I) atoms may either deposit randomly on the seed nanocrystals, form independent nanoclusters of a different size, or follow a combination of both processes. To determine which of these possibilities occurs requires a precise size separation method to follow both the cluster size distribution and the average cluster size. For very small changes in size between generations, TEM may be inadequate by itself, so we also analyzed the cluster

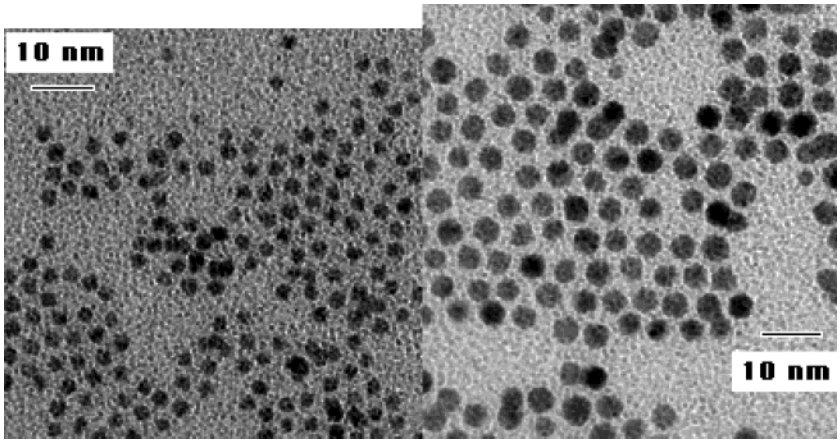

Figure 4. Left TEM shows the first generation of the growth experiment of Figure 3, with $D_c = 2.6 \pm 0.2$ nm, while the right TEM shows the following generation, with $D_c = 3.8 \pm 0.2$ nm.

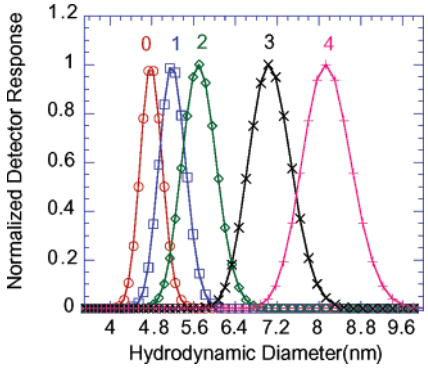

Figure 5. Normalized PDA detector response at 500 nm vs hydrodynamic diameter obtained by SEC for four generations of clusters, each serving as the seed for the growth of the next generation. The molar ratio of Au in the seed clusters to that deposited on their surface was 1:1.

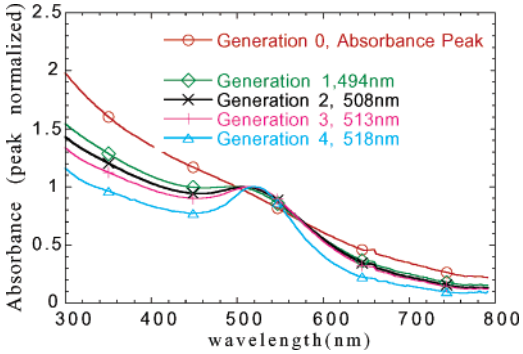

Figure 6. Absorbance spectra taken at the peak of the elution of each of the samples of Figure 5. Spectra have been normalized at an identical wavelength, 500 nm, to allow comparison of their shapes. The absorbance maximum wavelength is indicated in the legend.

sizes using SEC. Figure 3 shows the absorbance chromatograms of the seed and first two generations of particles grown from the $D = 1.8$ nm seed solution. We detect the cluster elution using the signal from the 500 nm wavelength element of the PDA. The indicated core sizes, D_c, in this figure were obtained by subtraction of the previously determined thickness of 2.5 ± 0.2 nm for the organic dodecanethiol passivating agent on the cluster surface.[7]

These core sizes are consistent with the sizes of the inorganic core as determined by TEM and shown in Figure 4.

Figure 3 shows cluster growth for the case of a 1:2 molar ratio of Au in the form of seed particles to atoms deposited for each generation grown. We anticipate that reducing this ratio to 1:1 will result in smaller increases in cluster sizes between generations. Figure 5 shows the SEC size characterization of each generation under these growth conditions. Generation 0 is the seed nanocluster solution grown by inverse micelle methods.

Examination of the spectra at the peak of the apex elution of Figure 5 and at the half-height positions shows that the spectral shapes throughout each elution peak are identical or homogeneous. This is a strong argument for both size and shape homogeneity of each generation, since the optical absorbance of Au nanoclusters is known to be strongly dependent on both size and shape. The growth of each generation is further confirmed by the development of an absorbance maximum for the larger clusters and its red shift with each generation as shown in Figure 6. The data in this figure was obtained from the PDA at the elution times shown in this figure.

An interesting effect is observed if we attempt to grow larger particles from the fourth generation whose SEC is shown in Figures 5 and 6. Namely, neither further red shift nor decrease in elution time (increase in time) is observed. This lack of further growth as shown in the TEM images of Figure 7 and may be due to an etching and size reduction which is known to occur for larger clusters in the presence of alkanethiols.[3]

If the ratio of atoms present as seed nanocrystals to atoms deposited is further increased from the 1:2 and 1:1 cases, slower growth is observed, as shown in the chromatogram of Figure 8. The ratio of total number of atoms in the seed nanocrystals to that deposited is 2:1 for each generation.

TEM analysis of generations 5−7 (elution peaks 6 and 7 not shown) for 1:2 growth in Figure 9 confirms that seed particles grow to produce sizes very similar to that observed for generations 3 and 4 in the 1:1 growth case. Again, it was difficult to grow sizes above ~6−8 nm using alkanethiols as stabilizers.

The number of atoms deposited onto the seed nanocrystals can be used together with the initial size of the seeds to control the final size of each generation. We tested the assumption that all the atoms are deposited onto the seeds under three growth conditions. The core sizes were obtained from TEM and SEC (Figures 3, 5, 8 and 9).

Assuming a spherical cluster shape and that all the injected atoms N_s (s = shell) are deposited heterogeneously onto the nanoclusters seeds with diameter D_c (c = core) which contain

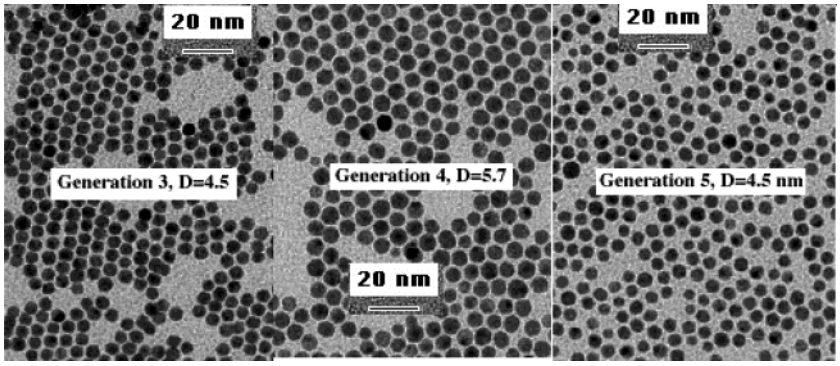

Figure 7. TEM at 50 kX magnification of generations 3−5 grown at a 1:1 ratio of Au seed nanocrystal atoms to Au feedstock atoms.

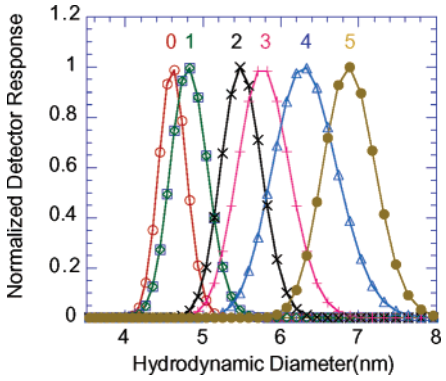

Figure 8. Normalized PDA detector response at 500 nm vs hydrodynamic diameter obtained by SEC for five generations of clusters, each serving as the seed for the growth of the next generation. The molar ratio of Au in the seed clusters to that deposited on their surface was 2:1. The starting nanocrystal solution (generation 0) consists of $D_c = 1.8$ nm seeds.

N_c atoms then, from mass conservation, the nanocluster final diameter, D_{c+s} can be computed from $(D_{c+s}/D_c)^3 = (N_c + N_s)/N_c$. We typically adjust our seed nanocrystal solution and organometallic feedstock to an identical atomic molar concentration, usually 0.01 M, and then control the ratio of the volume of the metal-organic feedstock atoms injected to the initial seed nanocrystal volume to control the number of atoms deposited in each growth generation. Generation j then serves as the seed population for generation $j + 1$. In Figure 10, we show the predicted sizes (solid lines) compared to sizes measured by SEC for three cases, $2N_m = N_f$, $N_m = N_f$, $N_m = 2N_f$. Generation 0 is the same initial $D = 1.8$ nm Au seed population from the three cases shown in Figures 3, 5, and 8.

Figure 10 demonstrates that most of the injected atoms are deposited onto the seed crystals in each case, the rate of growth being determined by the ratio of atoms in the form of clusters to those in the feedstock. There are deviations from the simple prediction for sizes larger than ~6 nm possibly due to etching effects of the thiols used to stabilize the clusters during the growth process. There is also a systematic deviation from the simple model for the slowest growth case, $N_m = 2N_f$. The clusters for generations 3 and greater are larger than expected which may imply some mass redistribution between clusters due to collisions and exchange of atoms. The results of Figure 10 are generally consistent with those of Lin et al., who studied Co nanocluster growth.[9]

Growth of Au on Ag Nanocrystals Seeds and Ag on Au Seeds. Any of the monodisperse growth generations whose sizes are shown in Figure 10 can serve as the starting point for deposition of other metals to form a core/shell type particle. Epitaxial growth is likely to be most successful for materials with the same lattice type (e.g., fcc) and similar atomic densities.

It is possible to dramatically alter the absorbance characteristics of metal nanoparticles by deposition of a shell of another metal onto its surface. Such fine-tuning of the color is potentially useful to create taggant materials (i.e., metal inks) which provide unique identification characteristics (e.g., in advanced anti-counterfeiting efforts). In such applications, even a complete knowledge of the particle atomic composition and size will not allow reverse engineering of the optical characteristics of the taggant, since the order of the growth sequence will determine its absorbance spectrum (e.g., a $D = 3$ nm particle Au/Ag with a 1:1 Au:Ag atomic ratio will differ in optical characteristics from an Ag/Au particle with the same composition, and both will differ in optical characteristics from a true alloy formed by simultaneous coreduction of the metal salts).[10] We demonstrate these differences in our Supporting Information Figure 3S.

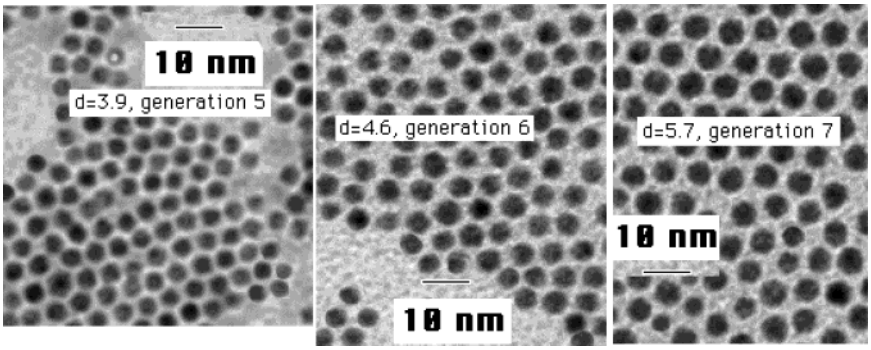

Figure 9. TEM images at 100 kX magnification of generations 5−7 grown at a 2:1 atomic ratio of Au seed nanocrystals to Au feedstock.

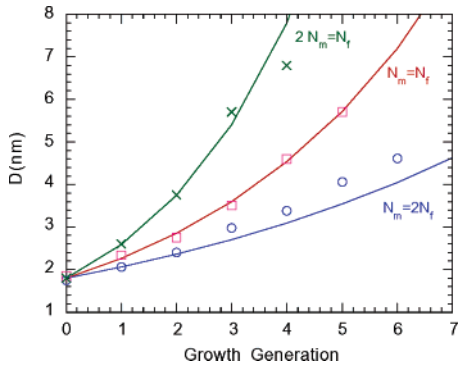

Figure 10. Cluster size vs growth generation for Au clusters. The solid curves are the predicted sizes assuming all N_f feedstock atoms deposit heterogeneously onto the N_m atoms in the form of nanocluster seeds. The symbols are the experimentally measured sizes from SEC and TEM.

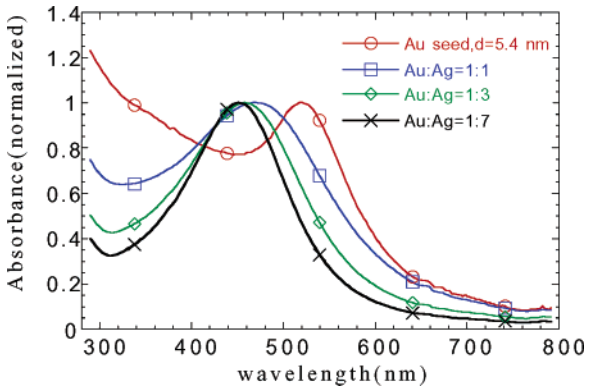

Figure 11. Effect of deposition of progressively larger amounts of Ag on Au nanoparticles with a core size of $D = 5.4$ nm. The atomic ratios of Au:Ag are indicated for each case. The ratios correspond to Ag shell thicknesses (total thicknesses) of ~1.4, 3.2, and 5.3 nm, respectively.

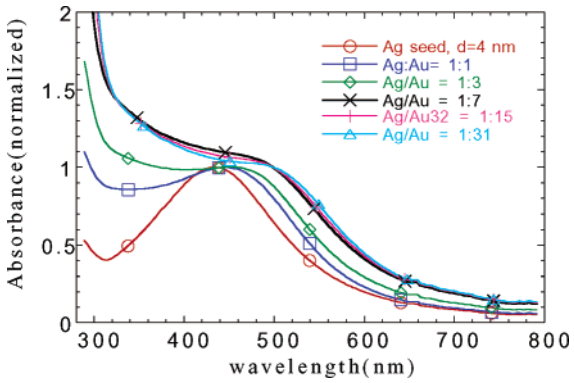

Figure 12. Effect of deposition of progressively larger amounts of Au on Ag nanoparticles with a core size of $D = 4.0$ nm. The atomic ratios of Au:Ag are indicated for each case. The ratios correspond to Au shell thicknesses (total thicknesses) of ~1, 2.5, 4, 6, and 8.2 nm, respectively.

We demonstrate the effect of Ag deposition on the absorbance properties of an Au nanoparticle with a $D = 5.4$ nm core in Figure 11. The red colored parent solution with an absorbance peak at 518 nm blue shifts in a systematic manner as thicker shells of Ag are formed around the core, ultimately resulting in a yellow colored solution with a narrower symmetrical plasmon typically associated with an Ag nanocluster.[9]

In the case of Au deposition onto Ag clusters, the absorbance peak shifts in the opposite manner, as shown in the example of Figure 12, where a seed population of $D = 4.0$ nm Ag was used. It is noteworthy that even when the particle has a 31:1 Ag:Au ratio which corresponds to a $D = 4$ nm Ag core with a total size of ~12 nm, the damping of the Au plasmon is much stronger than is observed in a pure Au particle of the same size.

In the Supporting Information, Figure 1S, we show the absorbance of a solution of $D = 5$ nm Ag and Au alloy clusters formed in a nonionic inverse micelle octane solution by simultaneous reduction of $HAuCl_4$ and $AgNO_3$. Two peaks at 425 and 505 nm with significant absorbance throughout this range were observed. We compared this to Supporting Information Figure 2S showing the results of the deposition of Au onto $D = 4$ nm Ag seeds, Figure 12, and Ag onto $D = 5.4$ nm Au seeds, Figure 11, for the 1:1 atomic ratio cases. The spectra for all three cases are distinct. In Supporting Information Figure 3S, we show an HRTEM micrograph of the Ag/Au particles with a 1:1 ratio of Ag:Au whose spectra is shown in Figure 10. Since both the lattice constant and density of Ag and Au are identical and they are miscible in all proportions, microscopy cannot unambiguously settle the issue of whether a core/shell or alloy formation occurs. The HRTEM shown in Supporting Information Figure 3S shows some particles with a core of 3−4 nm and a shell with a total thickness of ~1 nm, the dimensions measured depending on particle orientation.

IV. Discussion

In our experiments we found it necessary to remove the inverse micelles from the seed nanocrystal solution in order to ensure complete deposition of the feedstock atoms onto the seeds. However, Lin and co-workers demonstrated that this is not always necessary.[9] They grew successive generations of Co particles from seeds formed in cationic inverse micelles using the inverse micelle solution used to grow the seeds as the feedstock for each stage of growth. TEM size measurements showed the behavior we demonstrated in Figure 10. As in the present case, problems emerged in attempts to grow monodisperse particles much larger than 6−8 nm, as both homo- and heterogeneous growth occurred and resulted in bimodal size distributions. They did not attempt to control the rate of injection of the feedstock atoms to the degree possible with a programmable syringe pump as used in the present work but, nevertheless, achieved good results for the first few generations whose average size and dispersity were characterized by TEM. It would be worthwhile to repeat these experiments using an organometallic feedstock such as cobalt acetoacetonate in toluene using purified seeds as in the present work.

Growing larger particles by our slow injection method is limited by the stabilization and chemical interaction of the particular surfactants, alkanethiols, used in our studies. Apparently, the steric stabilization of the nanoclusters in the absence of the bulky nonionic and cationic surfactants used to synthesize the seed nanocrystals is inadequate. In fact, if 8−10 nm Au or Ag nanocrystals are first grown in a nonionic alkyl polyether surfactant which is sterically bulky and polydentite in character, the clusters are stable in solution for many years. However, in most cases, addition of even long chain alkanethiols to such solutions immediately results in aggregation of the clusters. So replacing the alkanethiol surfactants in the feedstock, with either ionic or cationic surfactants, may allow the growth process to continue to very large sizes.

Our experiments indicate that, beyond a size of ~6 nm, further addition of Au feedstock atoms in the presence of

alkanethiols leads to an etching and mass redistribution process. Such a process has already been demonstrated for thiolate stabilized 8−10 nm Au nanoparticles grown in nonionic inverse micelles.[3] It is very interesting to note that the same mechanism appears to be causing a size reduction in this case too.

In aqueous solution, growth of large size clusters in the range of 12−100 nm by a seeding technique using relatively monodisperse seeds has been demonstrated.[11−13] In these studies, however, the clusters were charge stabilized by the presence of citrate ions on their surfaces. This overcomes the requirement of bulky, polymer-like steric stabilizers to prevent particle agglomeration.

Because synthetic proceedures for producing monodisperse Ag seed nanocrystals are less well developed than for Au, there are no studies of the optical properties of Ag core particles with an Au shell. The existing work is either on alloys[14] produced via aqueous methods of co-reduction of metal salts or on core/shell particles of Au/Ag.[15,16] References 14−16 discuss the optical properties of larger, $D > 10$ nm, charge-stabilized colloids in water. Because of the difficulties of calculating optical properties of metal clusters with a charge on their surface, quantitative predictions for such colloids do not exist.[17] The small size of the sterically stabilized clusters produced by the present method also prevent direct comparisons to classical Mie theory.

The present results shown in Figure 11 are consistent with those found by Mallik and co-workers where 20 nm Au seeds particles with an absorbance resonance at 523 nm in water underwent a blue shift to ∼440 nm as increasing amounts of Ag were deposited.[16] Evidence of residual uncoated particles with a resonance absorbance peak at 523 nm were still observed in their solution, in contrast to the present case where all the Ag likely deposited onto the Au seeds.

(10) Wilcoxon, J. P. Metallic Quantum Dots: Preparation and Characterization. *Encylopedia of Nanoscience and Nanotechnology*; American Scientific Publishers: Jan. 2004 (available in print and on-line).
(11) Brown, K. R.; Walter, D. G.; Natan, M. J. *Chem. Mater.* **2000**, *12*, 306.
(12) Jana, N. R.; Gearheart, L.; Murphy, C. J. *Langmuir* **2001**, *17*, 6782.
(13) Pradhan, N.; Jana, N. R.; Mallick, K.; Pal, T. *J. Surf. Sci. Technol.* **2000**, *16*, 188−199.
(14) Link, S.; Wang, Z. L.; El-Sayed, M. A. *J. Phys. Chem. B* **1999**, *103*, 3529−3533.
(15) Mulvaney, P. *Langmuir* **1996**, *12*, 788−800.
(16) Mallik, K.; Mandal, M.; Pradhan, N.; Pal, T. *NanoLett* **2001**, *1* (6), 319−322.
(17) Kreibig, U.; Vollmer, M. *Optical Properties of Metal Clusters*; Springer-Verlag: Berlin, 1995.

V. Conclusions

We have demonstrated a method for the systematic growth of several generations of nanoparticles starting from a monodisperse seed population. The method relies on the slow coinjection of a metal-organic atom source and a reducing agent (a metal hydride) into a stirred solution of seed nanocrystals. In our experiments, each generation serves as a starting population for the next growth cycle. HRSEC and TEM were used to confirm that the deposition occurs only onto the seeds in a uniform manner, preserving the monodispersity of the parent sample.

We also showed examples of depositing Ag on Au nanocrystal seeds and Au on Ag nanocrystal seeds. In the former case, the absorbance characteristics were systematically shifted to the red and broadened in each generation having a thicker Au shell. In the case of the deposition of Ag on Au, a blue shift with larger shell thicknesses was observed, with the plasmon absorbance narrowing and becoming more symmetrical, characteristic of pure Ag nanoclusters.

This growth technique is general in the sense that a wide range of monodisperse metal nanoclusters may be synthesized using the inverse micelle method and can serve as seed populations for further heterogeneous growth. Also, a wide variety of metal organic precursors which are soluble in organic solvents such as toluene and benzene are available to provide atom sources for the heterogeneous deposition onto the seeds. Its chief limitation is that careful choice must be made of the passivating agent to permit growth of larger ($D > 6-8$ nm) clusters which require good steric stabilization. Moreover, such surfactants must still provide access to the cluster surface for deposition of additional atoms. We are presently investigating growth using polydentite stabilizers to extend our results to larger clusters.

Acknowledgment. This work was supported by the Division of Materials Science and Engineering, Office of Science, U.S. Department of Energy under Contract DE-AC04-AL8500. Sandia is a multiprogram laboratory operated by Sandia Corporation, a Lockheed−Martin Company, for the U.S. Department of Energy.

Supporting Information Available: Data plots and high-resolution TEM image. This material is available free of charge via the Internet at http://pubs.acs.org.

JA031622Y